JACS
JOURNAL OF THE AMERICAN CHEMICAL SOCIETY

COMMUNICATION

pubs.acs.org/JACS

Evolution of DNA Sequences Toward Recognition of Metallic Armchair Carbon Nanotubes

Xiaomin Tu,[†] Angela R. Hight Walker,[‡] Constantine Y. Khripin,[†] and Ming Zheng*[,†]

[†]Polymers Division and [‡]Optical Technology Division, National Institute of Standards and Technology, Gaithersburg, Maryland 20899, United States

ABSTRACT: The armchair carbon nanotube is an ideal system to study fundamental physics in one-dimensional metals and potentially a superb material for applications such as electrical power transmission. Synthesis and purification efforts to date have failed to produce a homogeneous population of such a material. Here we report evolutionary strategies to find DNA sequences for the recognition and subsequent purification of (6,6) and (7,7) armchair species from synthetic mixtures. The new sequences were derived by single-point scanning mutation and sequence motif variation of previously identified ones for semiconducting tubes. Optical absorption spectroscopy of the purified armchair tubes revealed well-resolved first- and second-order electronic transitions accompanied by prominent sideband features that have neither been predicted nor observed previously. Resonance Raman spectroscopy showed a single Lorentzian peak for the in-plane carbon−carbon stretching mode (G band) of the armchair tubes, repudiating the common practice of using such a line shape to infer the absence of metallic species. Our work demonstrates the exquisite sensitivity of DNA to nanotube metallicity and makes the long-anticipated pure armchair tubes available as seeds for their mass amplification.

The highly symmetric armchair single-wall carbon nanotubes (SWCNTs) occupy a unique position among carbon nanostructures. They preserve the linear energy dispersion of two-dimensional (2D) graphene at the Dirac point.[1] They are the only type to display true metallic character and are ideally suited for testing the Luttinger liquid behavior of one-dimensional metals.[2−4] Technologically, the late Richard Smalley regarded them as superb materials for electrical power transmission and championed the idea of using single-chirality armchair tubes as seeds to template their mass production (i.e., cloning).[5] Recent experimental work has shown the feasibility of the cloning idea,[6] and theoretical analysis has suggested the lowest growth activation barrier for the armchair type.[7] However, attaining homogeneous populations of single-chirality metallic species has proven to be an elusive goal. Here we report evolutionary strategies to find DNA sequences for the recognition and subsequent purification of two armchair species from synthetic mixtures. The new sequences were derived by single-point scanning mutation and sequence motif variation of previously identified ones for semiconducting tubes. Optical absorption spectroscopy of the purified armchair tubes revealed well-resolved first- and second-order electronic transitions accompanied by prominent sideband features that have neither been predicted nor observed previously. Resonance Raman spectroscopy showed a single Lorentzian peak for the in-plane carbon−carbon stretching mode (G band) of the armchair tubes, repudiating the common practice of using such a line shape to infer the absence of metallic species. Our work demonstrates the exquisite sensitivity of DNA to nanotube metallicity and makes the long-anticipated pure armchair tubes available as seeds for their mass amplification.

Single-chirality metallic tubes appear to be much more difficult to purify than their seminconducting counterparts. Indeed, the first purification of a single-chirality semiconducting tube species was reported as early as 2004,[8] and to date a few methods have been developed that can purify many different single-chirality semiconductor species.[9−11] Collectively as a distinct class of macromolecules, metallic tubes can be effectively separated from semiconducting tubes,[12−14] indicating a substantial difference between metallic and semiconducting tubes in their interactions with other molecules and external fields. Attempts have been made to purify single-chirality metallic armchair tubes. The best results achieved to date have yielded a mixture of several metallic armchair species,[15−17] suggesting much smaller physicochemical differences among different metallic species.

We have developed a single-chirality SWCNT separation method that exploits the strong interaction between single-stranded DNA (ssDNA) and SWCNTs.[13] DNA self-assembles onto SWCNT surfaces with a folding structure that is dependent on both the DNA sequence and the SWCNT chirality.[18,19] The resulting DNA−SWCNT hybrid can then be fractionated by anion-exchange chromatography (IEX). We previously devised a strategy to survey the vast ssDNA library in order to find specific sequences that enable IEX purification of particular (n,m) nanotube species from a synthetic mixture.[9] The survey was designed to span the maximum sequence space with a minimum number of test sequences via the use of simple nucleotide repeats. Out of >350 sequences tested, we were able to find only semiconducting tube recognition sequences in the 9−14-mer length range. Since these recognition sequences conform to the pattern of single purine/multiple pyrimidine repeats, it is reasonable to expect that recognition sequences for metallic tubes may be found outside the sequence space defined by the purine/pyrimidine repeats. However, the number of candidates remains astronomical, making identification of target sequences statistically improbable in the absence of an effective search strategy. In view of the structural similarities between metallic and semiconducting tubes, we decided to take an evolutionary approach to find metallic tube recognition sequences by limiting the candidate pool

Received: June 15, 2011
Published: July 21, 2011

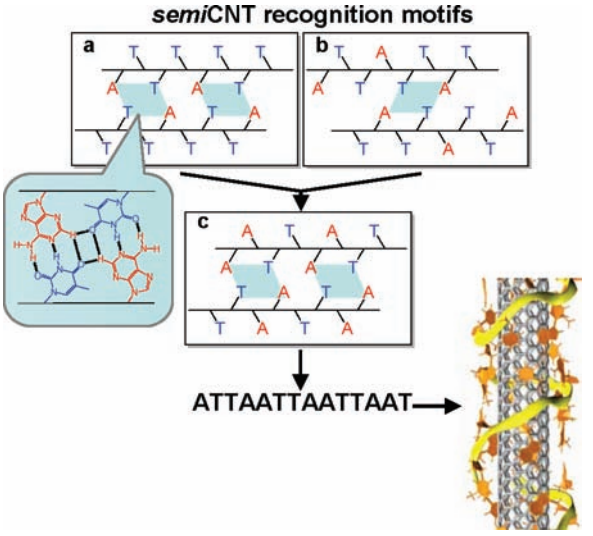

Figure 1. Sequence motif variation to derive a new sequence pattern for metallic tube recognition. The AATT repeats resemble previously identified ATT and ATTT repeats with the conservation of the A:T:A:T hydrogen-bonding quartets between adjacent strands (marked by the blue diamonds and shown in atomic detail in the callout panel) and the 2D sheet structure. This approach led to the identification of a (6,6) recognition sequence.

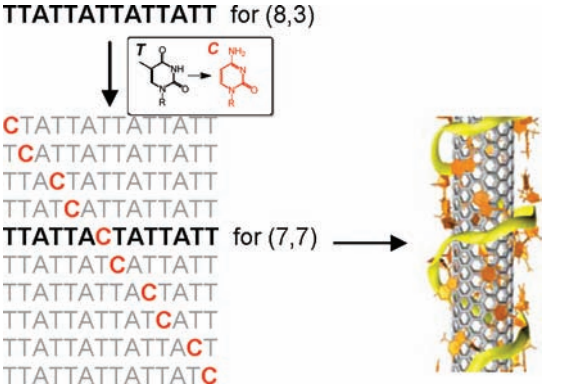

Figure 2. Single-point scanning mutation to evolve recognition sequences for metallic carbon nanotubes. Replacing thymines one at a time by cytosine in the semiconducting (8,3) recognition sequence TTATTATTATTATT resulted in the identification of the sequence TTATTACTATTATT that recognizes and enables purification of (7,7) nanotubes.

only to those that are direct descendants (as defined below) of semiconducting tube recognition sequences. Such an approach was expected to balance the need to deviate from the purine/pyrimidine pattern and the desire to conserve sequence features that are believed to sustain a 2D DNA sheet structure for ordered SWCNT wrapping.[9] Our evolutionary approach is analogous in spirit to the well-documented genetic algorithm for solving a wide variety of optimization problems.[20]

In one set of searches, we sought variations of the known sequence motifs. We noticed that many previously identified sequences are ATT and ATTT repeats. This empirical sequence selection rule was rationalized by a structure model we proposed that invokes interchain hydrogen-bonding interactions to form an ordered DNA wrapping sheet for SWCNTs.[9] As shown in Figure 1a,b, when nucleotide bases are placed on alternating sides of the backbone, interchain A:T:A:T hydrogen-bond quartets (blue diamonds in Figure 1) can be established between two adjacent antiparallel strands.[21,22] This model prompted us to test AATT repeats, which also form interchain A:T:A:T hydrogen-bond quartets (Figure 1c) and thereby conserve the 2D sheet feature of the ATT and ATTT repeats. The presence of two purines in the AATT repeats, however, deviates from the single purine/multiple pyrimidine sequence pattern for semiconducting tubes. In the length range of 9−14-mers, there are ~20 or so sequences that conform to the AATT repeat pattern. Through an exhaustive test of these sequences, we found that ATTAATTAATTAAT allows purification of (6,6) armchair tubes.

In another set of searches, we examined single-point mutations of previously identified sequences. We limited the mutation type to single-base purine-to-purine (i.e., A to G) or pyrimidine-to-pyrimidine (i.e., T to C) replacement. In most cases, mutation led to a loss of the original function [i.e., enrichment of a particular (n,m) species]. In some cases, either an improvement (i.e., higher yield and/or purity) or a complete switch in function was observed. In particular, a TTATTATTATTATT sequence was previously found to allow (8,3) purification, albeit with some metallic contamination.[9] A mutation scan replacing one T at a time by C (Figure 2) led to the identification of TTATTACTATTATT for (7,7) purification.

We used optical spectroscopy techniques to assign the structures of the purified nanotubes and reveal new spectral features. Absorption spectroscopy (Figure 3a) showed well-resolved first- and second-order electronic transitions for each of the two armchair tubes: M_{11} = 458 nm, M_{22} = 299 nm for (6,6); M_{11} = 505 nm, M_{22} = 312 nm for (7,7). The M_{11} values coincide with those reported in the literature[23] and thus support our structure assignment. The M_{22} values were measured for the first time for these two small-diameter armchair tubes. To analyze the dependence of measured M_{ii} values on the tube diameter d_t, we adopt the following scaling-law equation from ref 24 that includes a linear dependence of M_{ii} on $1/d_t$ arising from quantum confinement of the electronic structure of 2D graphene and a logarithmic correction that takes into account many-body effects:[25]

$$M_{ii} = a\frac{p}{d_t}\left(1 + b\log\frac{c}{p/d_t}\right)$$

where the zone-folding cutting line index p is equal to 3 and 6 for M_{11} and M_{22}, respectively, d_t is in nanometers, and a, b, and c are fitting parameters. Figure 3b shows that the scaling law using a = 1.120 eV nm, b = 0.507, and c = 0.816 nm^{-1} as the best values of the fitting parameters describes the measured data reasonably well. Accompanying each M_{11} transition is a weaker but well-resolved peak located at higher energy by 211 meV for (6,6) and 217 meV for (7,7), respectively (Figure 3c). This feature has not been reported previously for metallic tubes but resembles the ubiquitous phonon sidebands of the first electronic excitation in semiconducting tubes.[26] We attribute the slight asymmetry of the main M_{11} peak to the superposition of discrete and continuum exciton transitions that are 50−100 meV apart (Figure 3c), in line with theoretical predictions and experimental results obtained from single-tube measurements.[27,28]

Further confirmation of our structure assignment was provided by resonance Raman spectroscopy measurements. With 458 and 502 nm excitation, we detected in the radial breathing mode (RBM) region a single strong peak at 289 cm^{-1} for the

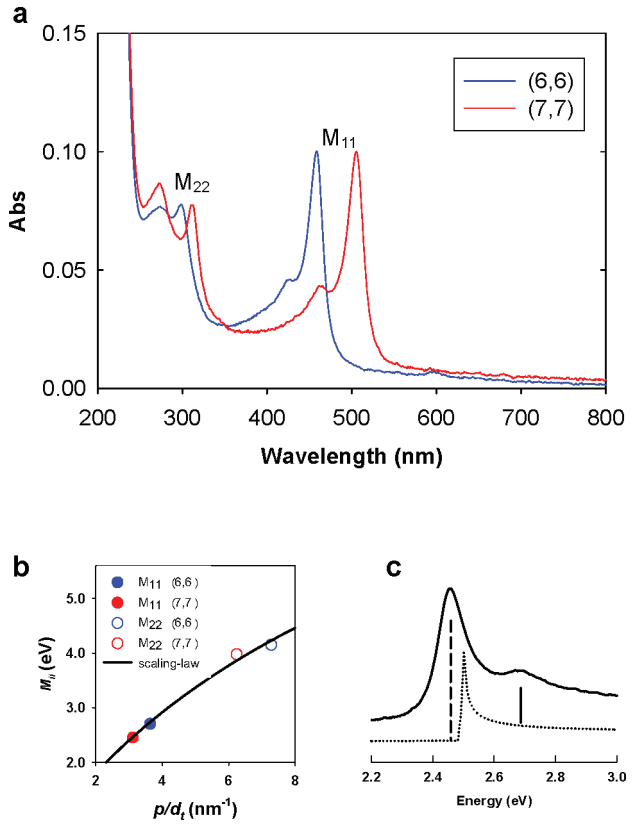

Figure 3. Optical absorption spectra and data analysis. (a) Optical absorption spectra of the purified DNA-wrapped (6,6) (blue) and (7,7) (red) armchair carbon nanotubes in water. The spectral intensities were rescaled for easy comparison, but no other processing steps (e.g., baseline subtraction) were done. (b) M_{ii} values as a function of p/d_t, where p = 3 and 6 for M_{11} and M_{22}, respectively, and d_t is the tube diameter in nm. The black solid curve is a fit to the scaling-law equation given in the text. (c) Line shape analysis of the M_{11} peak for (7,7) nanotubes (solid trace), which can be viewed as a superposition of three transitions: discrete (vertical dashed line) and continuum (dotted trace) exciton transitions and a sideband (vertical solid line) located 0.217 eV above the discrete exciton peak.

(6,6)-, and 250 cm^{-1} for the (7,7)-enriched fraction, respectively (Figure 4). These values are again consistent with reported RBM shifts for the two types of armchair tubes.[15,23] Excitations at other wavelengths (488, 514, and 632 nm) yielded no other unique RBM features. Most noteworthy is the G band (i.e., the in-plane carbon−carbon stretching mode) from each of the two metallic fractions, which shows a single, narrow, resonance-enhanced symmetric peak at 1582 cm^{-1} for (6,6) and 1587 cm^{-1} for (7,7). This observation is consistent with results obtained from single-nanotube measurements[29] and very recent measurements on a metallic-enriched nanotube mixture.[30] Our experiments on homogeneous populations of single-chirality armchair tubes, however, have removed the problem of limited statistical sampling associated with single-nanotube measurements and the possible contribution from semiconducting tubes in the nanotube mixture measurements. The symmetric (asymmetric) G-band line shape has been widely used to infer the absence (presence) of metallic tubes.[31−33] Our result shows that such a criterion is invalid for truly metallic armchair tubes.

In summary, we have designed and carried out an evolutionary procedure to identify DNA sequences that recognize and enable

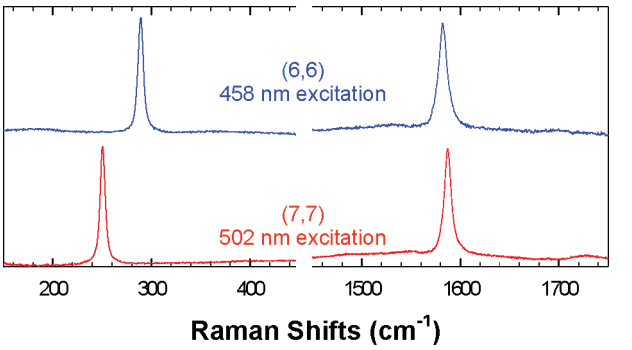

Figure 4. Resonance Raman spectra of purified DNA-wrapped (6,6) (blue) and (7,7) (red) armchair carbon nanotubes in the RBM and G-band regions.

the purification of armchair nanotubes, demonstrating the exquisite sensitivity of DNA sequences to carbon nanotube metallicity. While identification of the new sequences still relies on the trial-and-error method, our results certainly expand the existing database of recognition sequences and will undoubtedly contribute to the future discovery of sequence design rules through combined experimental and computational approaches. The availability of the long-sought-after single-chirality armchair tubes offers new opportunities for fundamental studies and application developments. In particular, cloning of armchair tubes, the success of which may have enormous technological implications, can now be tested using our purified materials as seeds.

Experimental methods. The SWCNT dispersion and separation in this work followed previously published procedures,[9] with the following modification. For dispersion, 1 mg of HiPco (Carbon Nanotechnologies, Houston, TX) or CoMoCAT SG76 (Southwest Nanotechnologies, Norman, OK) tubes was dispersed with 1.5 mg of DNA of a given sequence in 1 mL of sodium acetate buffer (0.1 M, pH 4.5) with 2 h of sonication. The dispersed mixture was incubated for 2 days before centrifugation to remove nondispersed bundles. IEX elution was done with a 2× SSC (0.3 M NaCl, 0.03 M sodium citrate)/0.5 mM EDTA/pH 7 and 0−1 M NaSCN gradient through an anion-exchange column (Biochrom, Terre Haute, IN). Into the purified fraction were then added 10 μg/mL free DNA corresponding to the sequence used for purification, 0.5 M NaCl, and 8% poly(ethylene glycol) (MW = 6 kDa). After overnight incubation, the pellet was collected after centrifugation and resuspended in 100 μL of water. This precipitation procedure concentrated the SWCNTs and at the same time removed residual amounts of graphitic impurities coeluted with the SWCNTs. This step was found to be necessary to reduce optical absorption from the impurities, thereby allowing resolution of SWCNT absorption features in the UV region. Typical yields corresponded to 100 μL at a concentration giving an optical density of 0.1 for M_{11} using a 1 cm path length, which is equivalent to sub-microgram quantities of SWCNTs. The average length of the purified armchair tubes was determined by atomic force microscopy to be ∼100 nm, which is considerably shorter than that of our purified single-chirality semiconducting tubes.

Resonance Raman spectra were collected with an Ar^+ laser (Coherent Innova Sabre) in a collinear, 180° backscattering configuration. A power of ∼15 mW was focused to a spot size of ∼100 μm within the liquid sample volume. The backscattered

light was collected with a triple-grating spectrometer (Dilor XY800) and a liquid nitrogen-cooled CCD detector with 300 s integration time averaged over three scans. The data were scaled and corrected by the subtraction of background signals from the NaSCN elution solution. Standard uncertainties of the optical measurements were determined by the instruments used: ±0.1 nm in the case of absorption spectroscopy and ±0.4 cm^{-1} for resonance Raman spectroscopy.

AUTHOR INFORMATION

Corresponding Author
ming.zheng@nist.gov

ACKNOWLEDGMENT

We thank Anand Jagota and Dan Roxbury for their help with figures and Jeff Fagan for discussions and experimental support.

REFERENCES

(1) Saito, R.; Dresselhaus, G.; Dresselhaus, M. S. *Physical Properties of Carbon Nanotubes*; Imperial College Press: London, 1999.
(2) Egger, R.; Gogolin, A. O. *Phys. Rev. Lett.* **1997**, *79*, 5082.
(3) Kane, C.; Balents, L.; Fisher, M. P. A. *Phys. Rev. Lett.* **1997**, *79*, 5086.
(4) Bockrath, M.; Cobden, D. H.; Lu, J.; Rinzler, A. G.; Smalley, R. E.; Balents, L.; McEuen, P. L. *Nature* **1999**, *397*, 598.
(5) Smalley, R. Remarks at 2005 Hope College Alumni Banquet. http://www.hope.edu/pr/pressreleases/content/view/full/7309 (accessed June 15, 2011).
(6) Yu, X.; Zhang, J.; Choi, W.; Choi, J.-Y.; Kim, J. M.; Gan, L.; Liu, Z. *Nano Lett.* **2010**, *10*, 3343.
(7) Ding, F.; Harutyunyan, A. R.; Yakobson, B. I. *Proc. Natl. Acad. Sci. U.S.A.* **2009**, *106*, 2506.
(8) Zheng, M.; Diner, B. A. *J. Am. Chem. Soc.* **2004**, *126*, 15490.
(9) Tu, X.; Manohar, S.; Jagota, A.; Zheng, M. *Nature* **2009**, *460*, 250.
(10) Ghosh, S.; Bachilo, S. M.; Weisman, R. B. *Nat. Nanotechnol.* **2010**, *5*, 443.
(11) Liu, H.; Nishide, D.; Tanaka, T.; Kataura, H. *Nat. Commun.* **2011**, *2*, 309.
(12) Hersam, M. C. *Nat. Nanotechnol.* **2008**, *3*, 387.
(13) Tu, X.; Zheng, M. *Nano Res.* **2008**, *1*, 185.
(14) Arnold, M. S.; Green, A. A.; Hulvat, J. F.; Stupp, S. I.; Hersam, M. C. *Nat. Nanotechnol.* **2006**, *1*, 60.
(15) Hároz, E. H.; Rice, W. D.; Lu, B. Y.; Ghosh, S.; Hauge, R. H.; Weisman, R. B.; Doorn, S. K.; Kono, J. *ACS Nano* **2010**, *4*, 1955.
(16) Sato, Y.; Yanagi, K.; Miyata, Y.; Suenaga, K.; Kataura, H.; Iijima, S. *Nano Lett.* **2008**, *8*, 3151.
(17) Green, A. A.; Hersam, M. C. *Nano Lett.* **2008**, *8*, 1417.
(18) Zheng, M.; Jagota, A.; Semke, E. D.; Diner, B. A.; McLean, R. S.; Lustig, S. R.; Richardson, R. E.; Tassi, N. G. *Nat. Mater.* **2003**, *2*, 338.
(19) Zheng, M.; Jagota, A.; Strano, M. S.; Santos, A. P.; Barone, P.; Chou, S. G.; Diner, B. A.; Dresselhaus, M. S.; McLean, R. S.; Onoa, G. B.; Samsonidze, G. G.; Semke, E. D.; Usrey, M.; Walls, D. J. *Science* **2003**, *302*, 1545.
(20) Holland, J. H. *Adaptation in Natural and Artificial Systems: An Introductory Analysis with Applications to Biology, Control, and Artificial Intelligence*, 1st ed.; MIT Press: Cambridge, MA, 1992.
(21) Mamdouh, W.; Dong, M.; Xu, S.; Rauls, E.; Besenbacher, F. *J. Am. Chem. Soc.* **2006**, *128*, 13305.
(22) Roxbury, D.; Tu, X.; Zheng, M.; Jagota, A. *Langmuir* **2011**, *27*, 8282.
(23) Fantini, C.; Jorio, A.; Santos, A. P.; Peressinotto, V. S. T.; Pimenta, M. A. *Chem. Phys. Lett.* **2007**, *439*, 138.
(24) Doorn, S. K.; Araujo, P. T.; Hata, K.; Jorio, A. *Phys. Rev. B* **2008**, *78*, No. 165408.
(25) Kane, C. L.; Mele, E. J. *Phys. Rev. Lett.* **2004**, *93*, No. 197402.
(26) Vora, P. M.; Tu, X.; Mele, E. J.; Zheng, M.; Kikkawa, J. M. *Phys. Rev. B* **2010**, *81*, No. 155123.
(27) Deslippe, J.; Spataru, C. D.; Prendergast, D.; Louie, S. G. *Nano Lett.* **2007**, *7*, 1626.
(28) Wang, F.; Cho, D. J.; Kessler, B.; Deslippe, J.; Schuck, P. J.; Louie, S. G.; Zettl, A.; Heinz, T. F.; Shen, Y. R. *Phys. Rev. Lett.* **2007**, *99*, No. 227401.
(29) Wu, Y.; Maultzsch, J.; Knoesel, E.; Chandra, B.; Huang, M.; Sfeir, M. Y.; Brus, L. E.; Hone, J.; Heinz, T. F. *Phys. Rev. Lett.* **2007**, *99*, No. 027402.
(30) Hároz, E. H.; Duque, J. G.; Rice, W. D.; Densmore, C. G.; Kono, J.; Doorn, S. K. 2011, arXiv:1101.1331v1 [cond-mat.mes-hall]. arXiv.org e-Print archive. http://arxiv.org/abs/1101.1331v1 (accessed June 15, 2011).
(31) Harutyunyan, A. R.; Chen, G.; Paronyan, T. M.; Pigos, E. M.; Kuznetsov, O. A.; Hewaparakrama, K.; Kim, S. M.; Zakharov, D.; Stach, E. A.; Sumanasekera, G. U. *Science* **2009**, *326*, 116.
(32) Krupke, R.; Hennrich, F.; Löhneysen, H. v.; Kappes, M. M. *Science* **2003**, *301*, 344.
(33) LeMieux, M. C.; Roberts, M.; Barman, S.; Jin, Y. W.; Kim, J. M.; Bao, Z. *Science* **2008**, *321*, 101.